arXiv:1409.6221v1 [cond-mat.mes-hall] 22 Sep 2014

Kondo effect in binuclear metal-organic complexes with weakly interacting spins

L. Zhang,[1,2] A. Bagrets,[1] D. Xenioti,[3,1] R. Korytár,[1] M. Schackert,[2] T. Miyamachi,[2,4] F. Schramm,[1] O. Fuhr,[1] R. Chandrasekar,[5] M. Alouani,[3] M. Ruben,[1,3] W. Wulfhekel,[2,1] and F. Evers[6,1]

[1] *Institute of Nanotechnology, Karlsruhe Institute of Technology (KIT), Germany*
[2] *Physikalisches Institut, Karlsruhe Institute of Technology (KIT), Germany*
[3] *Institut de Physique et Chimie des Matériaux de Strasbourg (IPCMS), Strasbourg, France*
[4] *Institute of Solid State Physics, University of Tokyo, Japan*
[5] *School of Chemistry, University of Hyderabad, India*
[6] *Institut für Theorie der Kondensierten Materie, Karlsruhe Institute of Technology, Germany*

(Dated: March 1, 2024)

We report a combined experimental and theoretical study of the Kondo effect in a series of binuclear metal-organic complexes of the form $[(\mathrm{Me(hfacac)_2})_2(\mathrm{bpym})]^0$, with Me = Nickel (II), Manganese(II), Zinc (II); hfacac = hexafluoroacetylacetonate, and bpym = bipyrimidine, adsorbed on Cu(100) surface. While Kondo-features did not appear in the scanning tunneling spectroscopy spectra of non-magnetic Zn_2, a zero bias resonance was resolved in magnetic Mn_2 and Ni_2 complexes. The case of Ni_2 is particularly interesting as the experiments indicate two adsorption geometries with very different properties. For Ni_2-complexes we have employed density functional theory to further elucidate the situation. Our simulations show that one geometry with relatively large Kondo temperatures $T_K \sim 10$ K can be attributed to distorted Ni_2 complexes, which are chemically bound to the surface via the bipyrimidine unit. The second geometry, we assign to molecular fragmentation: we suggest that the original binuclear molecule decomposes into two pieces, including Ni(hexafluoroacetylacetonate)$_2$, when brought into contact with the Cu-substrate. For both geometries our calculations support a picture of the (S=1)-type Kondo effect emerging due to open 3d shells of the individual Ni^{2+} ions.

I. INTRODUCTION

Molecular electronics holds the vision that functional electronic devices, like memory elements, rectifiers and transistors, may be realized by designing suitable molecular complexes. Over the past decade, two- and three-terminal molecular junctions with current-voltage characteristics resembling diod-,[1,2] transistor-[3–5] or memory-like[6,7] behavior have been demonstrated. The function of molecular devices can be extended using the spin degree of freedom initiating the field of molecular spintronics. An important step in this direction was made recently, when a giant magnetoresistance effect has been demonstrated for single molecules deposited on a ferromagnetic surface[8,9].

In order to achieve external control of electron spins, "spin-transition" complexes have been proposed, which can be addressed by temperature, pressure, light and presumably electron charging[10,11]. In these systems a *single spin* is the main protagonist. When it is brought in contact with a substrate, the Kondo-effect sets in. It has been observed in systems with increasing complexity ranging from 3d adatoms on metallic surfaces,[12,13] through molecules with extended π-orbitals,[15–18] to carbon nanotubes[19,20].

The motivation of our work is the question what happens if the molecule approaching the surface has *more* than a single active spin, say two exchange coupled spins that anticipates the case of single molecule magnets (SMMs)[21]. Interesting new aspects can enter already on the level of binuclear magnets[22] and arise from the competition of substrate-effects, such as Kondo-screening, and the inter-molecular exchange coupling.

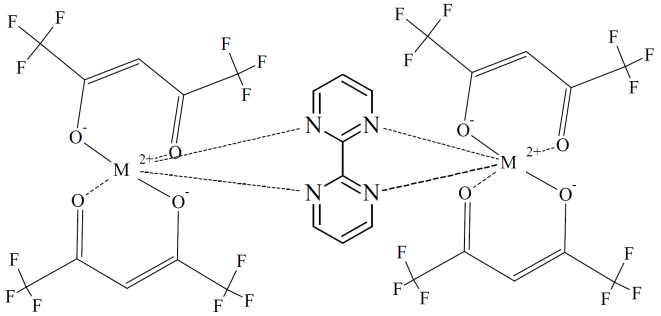


FIG. 1. Structure of the $(\mathrm{Me(hfacac)_2})_2(\mathrm{bpym})$ complex. Each metal ion Me^{2+} is linked with two hexafluoroacetylacetonate (hfacac) ligands by Me-O bonds. By forming N-Me bonds the aromatic 2,2'-bipyrimidine (bpym) ligand coordinates as bidentate chelate with two of the $\mathrm{Me(hfacac)_2}$ components.

Motivated by such a question, we have synthesized a series of binuclear metal-organic complexes of the form $[(\mathrm{Me(hfacac)_2})_2(\mathrm{bpym})]^0$, referred to later on as "Me_2" (see Fig. 1). These complexes have been deposited on a clean Cu(001) surface and studied with low-temperature scanning tunneling microscopy (STM). While no feature of the Kondo effect was found in the scanning tunneling spectroscopy (STS) spectrum of Zn_2 with closed shell 3d ions, an adsorption-site dependent zero-bias (Kondo) resonance was clearly resolved in the case of Mn_2 and Ni_2 molecules (see Fig. 2).

The Ni_2-case is particularly interesting, as the ad-

sorbed molecule appears in two variants that differ in STM-images and STS-characteristics. To rationalize these observations, we have performed calculations based on density functional theory (DFT). We thus identify possible adsorption geometries. Our simulations show that one observed geometry (with relatively large Kondo temperature T_K) can be attributed to the original Ni_2 complex with a distorted geometry bound to Cu(001) via the bipyrimidine (bpym) unit. The other is likely to arise from molecular fragmentation. We propose that upon approaching the substrate the molecule breaks and forms two Ni(hfacac)$_2$ moieties, which are then seen in the experiment.

II. SYNTHESIS AND CHARACTERIZATION OF BINUCLEAR COMPLEXES

Molecular geometries: The molecular structure of the neutral binuclear metal complexes $[(Me(hfacac)_2)_2(bpym)]^0$, with Me = Nickel(II), Manganese(II), Zinc(II); hfacac = hexafluoroacetylacetonate, and bpym = bipyrimidine, studied in this work is presented in Fig. 1. The structural details of the metal complexes, in particular the coordination environment of the metal ions, are sensitive to the kind of 3*d* metal ion involved (for details, see Supplementary Information,[31] Sec. IV). According to single crystal X-ray diffractometry each Mn^{2+} ion is situated in a distorted trigonal prismatic N_2O_4 coordination sphere leading to a Mn-Mn distance of 6.2 Å in Mn_2 dimer. By contrast, the Ni_2 complex exhibits a distorted octahedral coordination environment of each Ni^{2+}-ion[32] with a Ni-Ni distance of only 5.6 Å.

Magnetism: The magnetic behavior of polycrystalline samples of the Mn_2 and Ni_2 complexes was determined between 2 K and 300 K (Supplementary Information,[31] Sec. IV). At room temperature Mn_2 has a $\chi_M T$ value of 9.03 cm^3·K·mol^{-1} (here χ_M is the molar magnetic susceptibility and T is the temperature), corresponding to two uncoupled high-spin Mn(II)-ions with a spin value of S=5/2 each, while Ni_2 shows a $\chi_M T$ product of 2.23 cm^3·K·mol^{-1}, corresponding to two uncoupled Ni(II)-ions with S=1. Between 300 K and 75 K both the Mn_2 and Ni_2 complexes show paramagnetic behavior, while below 75 K weak antiferromagnetic (AF) behavior sets in. The AF exchange interaction between the two divalent 3*d* ions through a bpym bridging ligand is reported as $J_{ex}^{AF} = 1.6$ meV[33] and $J_{ex}^{AF} = 2.06$ meV[32] for Ni_2, which is about 10 times larger than the exchange interaction observed in Mn_2 with $J_{ex}^{AF} = 0.13$ meV.

DFT-calculations for the Ni_2 complex: The spin state of each of the two Ni(hfacac)$_2$ units was determined as $S = 1$ assuming an [Ar]$3d^8$ electronic configuration for Ni^{2+} ion. Specifically, the atomic structure of the non-adsorbed (gas-phase) Ni_2 complex was refined starting form the X-ray diffraction structure with Ni^{2+} ions in distorted octahedral environment (see Supplementary Information[31], Sec. I, for computational details). The results of the "constrained" DFT calculations are summarized in the first row of Table I. In particular, our calculations predict a "singlet" ground state with the two spins, S=1, coupled antiferromagnetically. For the gas-phase complex, very low excitation energy ($\simeq$ 15 meV) is observed with an excited state exhibiting ferromagnetic coupling. Our results are consistent with experimental findings: weak antiferromagnetic exchange interaction between the two metal ions of the $[(Me(hfacac)_2)_2(bpym)]^0$ complexes facilitated by the bpym ligand has been reported before[32].

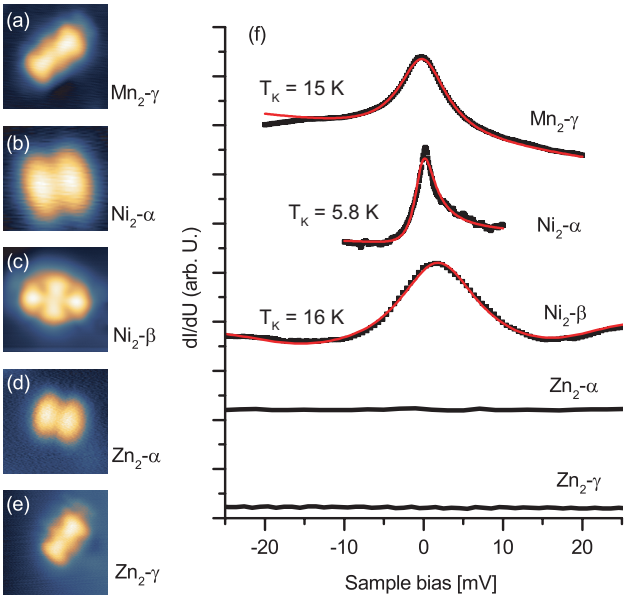


FIG. 2. Topography of (a) Mn_2-γ, (b) Ni_2-α, (c) Ni_2-β, (d) Zn_2-α, and (e) Zn_2-γ (images a-e are squares of side length of 3.7, 2.8, 2.5, 2,9, and 3.3 nm, respectively. Feedback conditions are 100 mV and 1 nA, 200 mV and 200 pA, −10 mV and 200 pA, 15 mV and 1 nA, 100 mV and 1 nA, respectively). The orientation of β and γ configuration follows [001] and [011] direction of the substrate, respectively, while the orientation of α configuration seems to be random. The differential conductance dI/dU near the Fermi-level is shown in (f). The black dots are experimental data which were fitted with Fano-functions (red lines). The STM images and STS were measured at 4.2 K. The spectra are normalized and a linear background was considered to obtain reasonable fitting result.

III. STM EXPERIMENTS

The STM experiments were performed using a home-built, low-noise STM operating between 0.7–4.2 K in ultra-high vacuum (UHV) ($p < 10^{-9}$ mbar)[34]. Clean and atomically flat Cu(100) substrates were prepared *in situ* followed by deposition of molecules by sublimation at 80–100 °C. Three adsorption configurations, α (Ni_2 and Zn_2), β (only Ni_2) and γ (Mn_2 and Ni_2), of the molecules

on Cu(100) were found (see Fig. 2a-e). Scanning tunneling spectroscopy (STS) measurements were performed on these different configurations. Kondo-like peaks were clearly resolved in the dI/dU curves of Mn_2 and Ni_2 (in both configurations) near the Fermi-level while no remarkable feature was found in the dI/dU curve of the non-magnetic Zn_2 complexes (see spectra displayed in Fig. 2f).

The Kondo-effect arises when the magnetic moment of an impurity is screened by surrounding electrons of a nonmagnetic substrate[35,36]. As the simplest manifestation of the interaction between the localized spin and delocalized electrons, the shape of the zero bias anomaly in STS caused by the Kondo-effect can be described by a Fano resonance[37–39]:

$$\frac{dI}{dU}(U) \propto \frac{(\varepsilon + q)^2}{1 + \varepsilon^2}, \tag{1}$$

where

$$\varepsilon = \frac{eU - \varepsilon_0}{\Gamma}, \tag{2}$$

and ε_0 is the energy shift of the resonance from the Fermi-level, Γ is the width of the resonance. The Fano parameter q characterizes the interference of tunneling between the tip and the magnetic impurity and tunneling between the tip and the sample[40]. Considering the temperature dependence, the Kondo-resonance can be approximated by a Lorentzian resonance[41]. Thus the energy width $2\Gamma(T)$ (full width at half maximum) of a Kondo-resonance can be expressed as:

$$2\Gamma(T) = 2\sqrt{(\pi k_B T)^2 + 2(k_B T_K)^2}, \tag{3}$$

with k_B being the Boltzmann constant, T being the environment temperature, and T_K being the Kondo-temperature. By fitting the experimental STS with equations (1)–(3), the Kondo-temperature T_K is extracted.

The Zn^{2+} ions in the complex are expected to have a full $3d$ sub-shell, so a magnetic moment is absent. This is in agreement with the SQUID measurements of the crystals of this complex. Thus, a Kondo-effect could appear only in adsorbed molecules if a charge transfer between the molecule and the substrate leads to the acquisition of a magnetic moment on the molecule. Since our measurement do not indicate a Kondo-resonance (compare Fig. 2f), we conclude that the interaction with the substrate is too weak for such a charge transfer. Contrary to Zn^{2+}, in Mn_2 and Ni_2 the central Mn^{2+}/Ni^{2+} ions exhibit a partially filled $3d$ shell and therefore carry a finite magnetic moment. They are at the origin of the Kondo-effect that we observe in our measurements, Fig. 2. By fitting to the Fano-shaped resonance, a Kondo-temperature of 15 K for Mn_2 is determined.

With Ni_2 the situation is more complex since two different adsorption geometries (referred to as α and β) are observed, see Fig. 2b,c. We determine two Kondo-temperatures, 5.8 K and 16 K for Ni_2-α and Ni_2-β, respectively. An even clearer difference between these adsorption geometries exhibits itself in a site-dependent STS measurement that we perform on Ni_2-α and Ni_2-β, see Fig. 3. The measurement shows that the Kondo-resonance has a single maximal amplitude at the center of the Ni_2-α complex (cf. Fig. 3a,c), while two spots with maximal amplitude of dI/dU signal separated by a distance of 4 Å are clearly resolved in the STS map of Ni_2-β (cf. Fig. 3b,d), which match with the two Ni^{2+} ions and their expected distance in the molecule.

At first sight, these results suggest that adsorption configurations of Ni_2-complexes may look like shown in Fig. 3(e,f). Namely, Ni_2-β could correspond to the molecular complex, which 'lies' on the surface with both of its hfacac ligands, thus exposing the two Ni ions seperately to the STM tip. The α-configuration could correspond

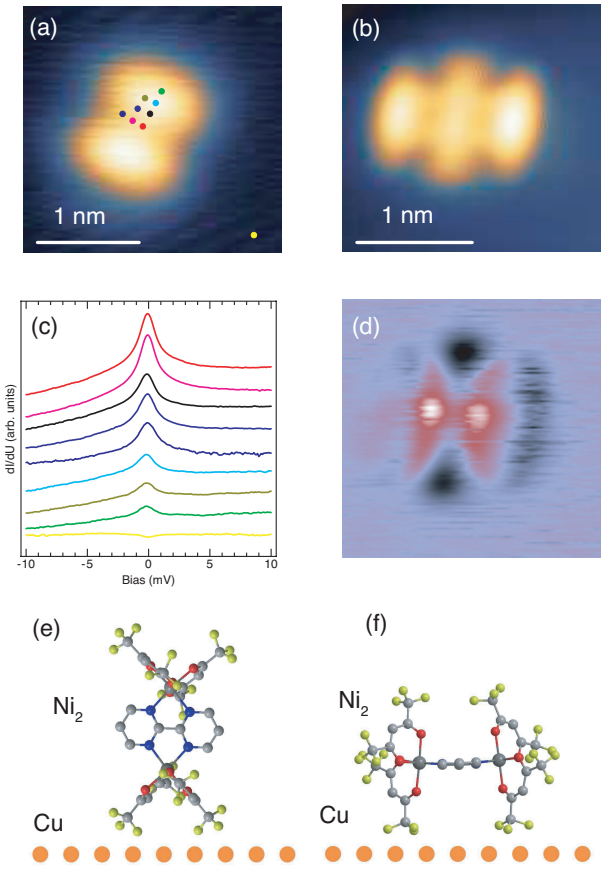


FIG. 3. Topography of Ni_2-α (a) and Ni_2-β (b). STS on different position of the Ni_2-α is shown in (c) ($T = 1$ K, feedback conditions: $U = 10$ mV, $I = 20$ nA, 200 μV modulation). STS (dI/dU) map of Ni_2-β is shown in (d). White areas indicate large differential conduction, black low. ($T = 5$ K, feedback conditions $U = 10$ mV, $I = 10$ nA). An intuitive assumption for the adsorption configurations of Ni_2-α and Ni_2-β (front view) on the Cu(100) substrate is shown in (e) and (f), respectively.

to the complex, which 'stands' on the surface with one hfacac ligand and the other hfacac ligand is seen in its topographic image. This would expose the two Ni ions above each other such that a single Kondo-resonance is observed in STS. As we show later on, the latter assignment is inconsistent with the theoretical considerations. Below, we propose an alternative scenario.

IV. THEORY

To elucidate microscopic details of the Kondo-effect observed experimentally, we have performed elaborated DFT calculations. Our main objective is to understand the dependence of the Kondo-resonance of the Ni_2 complex on the adsorption site. Additional questions that we address will concern the nature of the molecular orbitals involved in the interaction with conduction electrons, and how delocalized electrons compete for screening of the initially antiferromagnetically coupled spins.

A. Simple adsorption geometries

We analyze the adsorption geometries schematically illustrated in Fig. 3(e,f). They exhibit gas-phase Ni_2 complexes placed on Cu(001) surface (see Supplementary Information,[31] Sec. IIA, for computational details). Our simulation results indicate fluorine-copper distances above $\sim$ 3 Å. This distance implies that a weak van-der-Waals (vdW) force dominates binding to the surface. There is only a weak hybridization between molecular and substrate states, which translates into narrow molecular resonances, $\Gamma \simeq 10$ meV, as seen from the spectral function $A(E)$ projected on the Ni(II) ion (see Supplementary Information,[31] Suppl. Fig. 2). Giving typical parameters of the Anderson model read from $A(E)$, namely, single occupied resonance level width $\Gamma \simeq 10^{-2}$eV, on-site Coulomb repulsion energy $U \sim 2$eV, and position of the resonance level $\varepsilon_d \sim U/2 \sim 1$eV relative to the Fermi-energy, we can estimate the Kondo-temperature as[44,45]

$$k_B T_K \sim U\sqrt{\frac{\Gamma}{4U}}\, e^{-\pi U/4\Gamma} \sim 0.1\, e^{-10^2\pi/2} \text{ eV} \sim 10^{-69} \text{ eV}.$$

This result is contradicting the experimental finding of $k_B T_K \sim 10$ meV, so that we exclude adsorption geometries shown in Figs. 3(e,f). Alternatives should allow for a stronger binding with a significant amount of hybridization in order to achieve larger Γ-values.

B. α-configuration: Ni(hfacac)$_2$ fragments on Cu(001)

In order to enforce a much larger coupling of the molecular complex to the substrate we first consider the extreme case of molecular fragmentation, see Fig. 4a. Here we include the possibility that coordination bonds between Ni^{2+} ion and nitrogen atoms are broken, and a Ni(hfacac)$_2$ moiety, which is chemically bound to a Cu surface, is observed in the experiment. In that situation the coupling of the spin to the Cu surface is comparable to the case of single Ni adatom (no ligands attached), and drawing from related earlier experimental experience[12–14] one might suspect Kondo-temperatures of the order of tenth of meV roughly consistent with the present measurements. In order to show that the fragmentation scenario is consistent with the experimental findings, we observe following facts:

(i) *Simulated STM-images.* Our simulations of fragmented molecules (Fig. 4d,e) yield STM-images reproducing the most important characteristics of the experimental ones for Ni_2-α: the outermost contours have a butterfly shape, two mirror planes exist, the size of experimental and computational images are consistent. It is encouraging to see that also non-trivial details are (partially) reproduced. Namely, theory predicts a non-zero optimal angle, 45° (Fig. 4b) that fixes orientation of the fragment's mirror planes *vs* the fcc [100] direction of the (001) surface plane (see also Supplementary Information,[31] Suppl. Fig. 3). A non-zero angle, $\approx 20°$, is

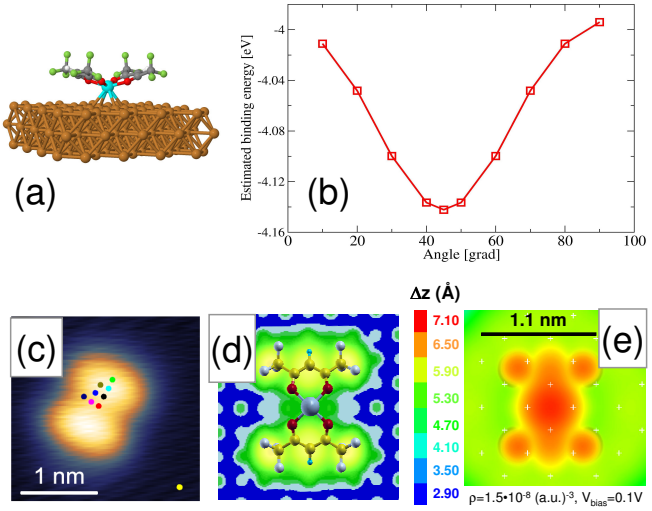


FIG. 4. (a) Ni(hfacac)$_2$ moiety bound to a Cu(001) surface via a Ni atom placed at the *hollow* site. (b) Estimated dependence of the binding energy of Ni(hfacac)$_2$ to Cu (001) surface on the angle that fixes the orientation of the moiety's mirror planes *vs* the [001] direction of the fcc (001) surface. (c) Experimentally recorded Ni_2-α STM image (reproduced from Fig. 2). (d) Simulated image of Ni(hfacac)$_2$, computed employing VASP package[47]: different colors refer to isosurfaces of the space-resolved (local) density of states (DoS) at the Fermi-level. (e) Simulated image of Ni(hfacac)$_2$, computed employing AITRANSS package[48,49]: selected three-dimensional isosurface of the space-resolved DoS (above the molecule) integrated over the energy window 0.1 eV around the Fermi-level is shown, where color coding refers to the distance Δz to the Cu surface. In consistent with experimental STM image, simulated images obey two mirror planes and outermost contours with a butterfly shape.

TABLE I. Relative energies of the low-energy spin configurations realized in Ni_2 complexes, which were estimated based on the ground state constrained DFT calculations (see Suppl. Information[31] for computational details). Considered molecules are: (i) gas-phase relaxed Ni_2 complex, with Ni^{2+} ions found in distorted octahedral environment (Suppl. Fig. 1a); (ii) free but distorted Ni_2 complex, pre-relaxed in the presence of Cu surface, where local C_{2v} symmetry has been kept (Suppl. Fig. 4a); (iii) free but distorted Ni_2 complex, relaxed in the presence of Cu surface where symmetry constrains have been released (Suppl. Fig. 4b). Spin configurations labeled as F and AF stand for ferromagnetic (F) and antiferromagnetic (AF) coupling, respectively, between $S = 1$ spins localized on Ni^{2+} ions. Last column refers to magnetically excited zero-spin (closed-shell) state at one of Ni^{2+} ions.

	DFT implementation	AF: $\uparrow\uparrow$ $\downarrow\downarrow$	F: $\uparrow\uparrow$ $\uparrow\uparrow$	$\uparrow\uparrow$ $\uparrow\downarrow$
(i) relaxed Ni_2	FHI-aims[42]	0.000 eV	15.8 meV	0.500 eV
complex	TURBOMOLE[43]	0.000 eV	14.9 meV	0.522 eV
(ii) distorted Ni_2 complex	FHI-aims	0.000 eV	6.9 meV	0.396 eV
with C_{2v} symmetry	TURBOMOLE	0.000 eV	6.1 meV	0.390 eV
(iii) distorted	FHI-aims	0.000 eV	2.5 meV	0.456 eV
Ni_2 complex	TURBOMOLE	0.000 eV	1.9 meV	0.361 eV

also observed in the representative experimental images of Ni_2-α (see Suppl. Fig. 5).

(ii) *Spatial dependency of Kondo-amplitude.* The fragment's geometry is such that the associated Kondo-resonance would have maximum amplitude with the STM-tip located in the center of the image (at Ni atom). That is in consistent with the structure of the spatially resolved Kondo-resonance of Ni_2-α observed experimentally (cf. Fig. 2a,c).

(iii) *The effect of temperature on the adsorption.* Experimental STM images characterizing adsorption of Ni_2 complexes on Cu(001) surface (Suppl. Fig. 5) suggest that molecular fragmentation at surface is likely triggered by the temperature. Namely, experimental data (Suppl. Fig. 5) reveal that when Ni_2 complexes are evaporated on the substrates at room temperature, two species – Ni_2-α and Ni_2-β – are found, while Ni_2-α, which we attribute to molecular fragments, is not found after deposition onto pre-cooled substrates (77K).

Since the fragmentation scenario is consistent with the experimental phenomenology, we perform further *ab initio* calculations with the goal to better understand the molecular magnetism and eventually estimate the Kondo-temperature.

We consider the atomic configuration of Ni atom as $[Ar]4s^2 3d^8$. In the simplified picture of a free $Ni(hfacac)_2$-fragment, the $4s$-states hybridize so strongly with the ligands, that the s-electrons are effectively transferred to ligand orbitals. Therefore, the metal ion takes the Ni^{2+}-configuration and exhibits two unpaired spins. We performed a DFT-study within the generalized gradient approximation (GGA, PBE exchange-correlation functional[50]) of the molecule in gas-phase (for details, see Supplementary Information,[31] Sec.I). Our results confirm above picture: we find a spin-polarized ground state with a magnetic moment of $2\mu_B$. The magnetization is largely due to two orbitals (a and b on Fig. 5) that are populated with up-spin electrons, only, and that contribute substantial weight to both Ni d_{z^2} and d_{xy} atomic states.

One may ask whether the fragment keeps its magnetic moment when adsorbed on the substrate. To answer this question, we performed another spin-DFT study, whose details are presented in the Supplementary Information[31] (Sec.II and Suppl. Fig. 3). In essence, the substrate further breaks the residual degeneracy of the d-orbitals splitting d_{z^2} and d_{xy} by 1.4 eV. As a result, d_{z^2} is nearly full (0.4 eV below E_F), while d_{xy} is nearly empty (1 eV above E_F with resonance $\Gamma_b \approx 10^{-2}$eV). The magnetization drops after adsorption by about a factor of two, down to 1.2 μ_B. The net charge(electron)-transfer to the molecule in the adsorption process is $0.4e$.

The GGA-type calculation leaves us with a situation where a localized $3d_{z^2}$-type orbital is only partially occupied. In DFT with conventional local exchange-correlation (XC) functionals (LDA, GGA) this is typically an indication of correlation physics, such as the Coulomb-blockade. The Coulomb-blockade is not described by conventional DFT-functionals, but it can be captured on the level of GGA+U.[51,52] Therefore, following Ref. 55, we performed a GGA+U calculation placing a repulsive on-site term with (relatively large) strength $U = 6$ eV on the metal site. (Details of our implementation are given in Ref. 56.) The interaction shifts the spin-down resonance a from 0.4 eV below to 0.5eV above E_F (Fig. 5). Hence, the magnetic moment increases up to 1.62 μ_B thus suggesting the picture of the (S=1) Kondo-effect.

So far our *ab initio* study has ignored the spatial structure of the two molecular orbitals involved, orbital a with substantial contribution from Ni d_{z^2} atomic state, and orbital b with substantial contribution from Ni d_{xy} atomic state. These molecular orbitals are depicted in Fig. 5. As can be seen, the a-orbital (first quantum dot, Γ_a) is directed towards the surface. Hence, it hybridizes with the substrate much stronger than the b orbital (second dot Γ_b), i.e. $\Gamma_b \ll \Gamma_a$. Each level has a single occupancy and the electrons populating them are coupled ferromagnetically. Since the exchange interaction (~ 0.5 eV, see

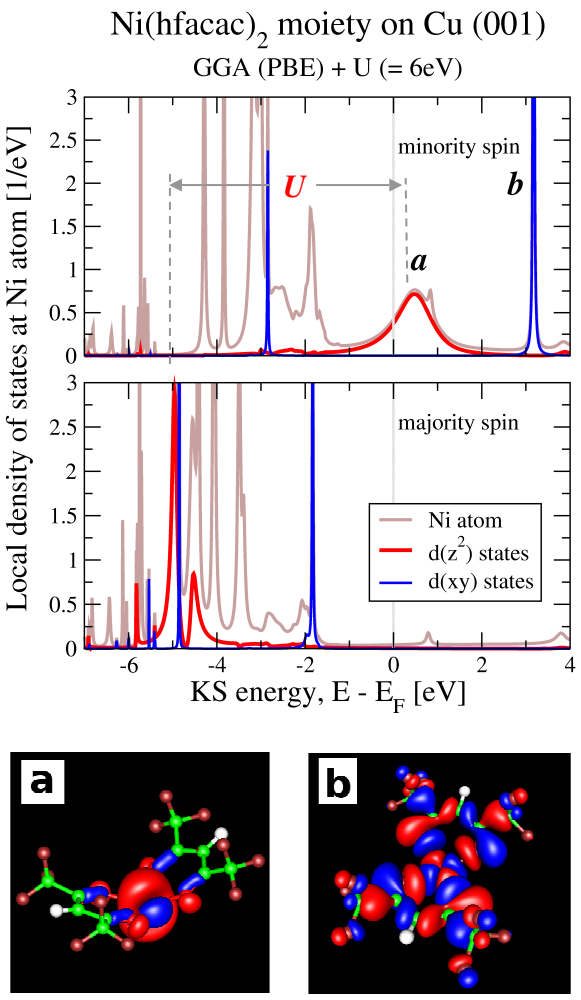


FIG. 5. Upper plot: spin dependent local density of states projected on Ni atom of the $Ni(hfacac)_2$ on Cu(001). Red and blue lines highlight contributions to the LDOS associated with Ni d_{z^2} and d_{xy} orbitals. Lower plots: corresponding Kohn-Sham wave functions of the free standing molecule.

Table 1) is much larger compared to the expected Kondo energy scale $\sim$ 10 K, both spins form a triplet, $S = 1$. Reading parameters from the spectral function (Fig. 5),

$$\Gamma_a \simeq 0.8 \text{ eV} \gg \Gamma_b;\ \varepsilon_d \simeq 0.5 \text{ eV};\ U \simeq 5.5 \text{ eV} \gg \varepsilon_d,$$

and using a formula[44,45] for the Kondo-temperature,

$$k_B T_K \simeq 0.41\, U \sqrt{\frac{\Gamma^*}{4U}}\, e^{-\pi\varepsilon_d/\Gamma^*}, \qquad (4)$$

where $U \gg \varepsilon_d$ and $\Gamma^* = \Gamma_a/2$ for the case of double-dot system, we obtain $k_B T_K \simeq 5.84 \times 10^{-3}$ eV, i.e. a Kondo-temperature $\simeq$ 70 K in qualitative agreement with the experiment.

We emphasize that a more precise estimation of the Kondo-temperature is hampered by exponential dependence of T_K on model parameters. For example, taking into account that DFT has a tendency to overestimate resonance line-widths, we may assume a slightly smaller $\Gamma_a \simeq 0.6$ eV. This reduces T_K down to $\simeq$ 16 K, which is in good agreement with the experimentally observed value.

C. β-configuration: distorted Ni_2 complex on Cu(001)

Spatially resolved intensity of the Kondo-resonance, measured on top of Ni_2-β image (Fig. 3d) suggests that also molecular species with two metal ions are to be found on a Cu surface. To rationalize this observation, we performed numerical simulations, to find an intact but strongly distorted molecular conformation (see Fig. 6g) that establishes a chemical bond to the Cu surface — an important prerequisite for observable Kondo-temperatures. This bond is presumably realized via the delocalized π-orbitals of the central bpym unit overlapping with the electron density extending from the surface. The bond involves contributions of the vdW forces, which have been accounted for in our simulations, and presumably has ionic character due to fractional charge transfer to the quasi-degenerate LUMOs[54].

We mention that even for the modern *ab initio* methods, finding the relaxed ground state structure of a large organic molecule (such as Ni_2 complex) on a surface is a non-trivial procedure. Due to the many atomic degrees of freedom involved, relaxation can end up in different molecular conformations with energies differing by $\sim$ 100 meV, as was also the case in our simulations. To be specific in the following discussion, we focus on two representative but slightly different conformations of "distorted" Ni_2 complex (for details, see Suppl. Fig. 4).

The first conformation (see Suppl. Fig. 4a) has been obtained within the preliminary DFT relaxation procedure: the atomic structure of the complex has an (approximate) C_{2v} symmetry, in registry with the underlying fcc(001) surface. For this conformation, the simulated STM image of the complex reveals a "cross-like" structure, resembling Ni_2-β experimental images (see Fig. 6a,c,e). Further relaxation steps within the simulation account for an energy gain of about $\sim$ 0.25 eV: the local symmetry of the molecular complex is broken resulting in the second conformation (see Suppl. Fig. 4b). Then formerly symmetric simulated "cross-like" STM images are transformed to the ones with broken symmetry (cf. Fig. 6d,f), which were also experimentally observed (cf. Fig. 6b).

The structure of the binuclear complex suggests that the molecular spins should reside on the $Ni(hfacac)_2$ units, where each unit could accept two unpaired electrons (referred to as S=1) owing to [Ar]$3d^8$ electronic configuration of the Ni^{2+} ion. Essentially, the two S=1 subsystems are magnetically nearly decoupled, since only a weak indirect ("super-exchange") interaction between them could be realized via the π-orbitals of the bpym

unit. Thus, we anticipate that each subsystem will develop a Kondo-effect, independently, as the molecular complex provides two parallel conduction paths (channels) for the tunneling electron, one for each spin.

These expectations are fully confirmed by our computational analysis. Constrained DFT calculations (see data in Table 1) predict a "singlet" ground state with antiferromagnetically (AF) coupled S=1 spins. For the distorted Ni_2 complex, the state with ferromagnetically (F) coupled S=1 spins is only $\sim$ 2 meV above the AF state.

The frontier molecular orbitals (see Fig. 7, bottom panels) carry unpaired spins (ferromagnetic coupling between S=1 subsystems is considered there) confirming the above picture: two out of four orbitals, a and b, are primarily localized on the "left-hand" side of the Ni_2 complex, while their counterparts, a' and b', are localized on the "right-hand" side. When the Ni_2 complex is brought in contact with the Cu surface, these molecular orbitals are transformed to resonances (a,b,a',b') in the spectral function centered around -1.5 eV below the Fermi-level E_F (see Fig. 7), while the upper Hubbard band (ε_d) is placed just above E_F. Furthermore, since the wave functions a and a' involve larger contributions from π orbitals of the central bpym unit, the corresponding resonances a and a' are much broader than the b and b' ones.

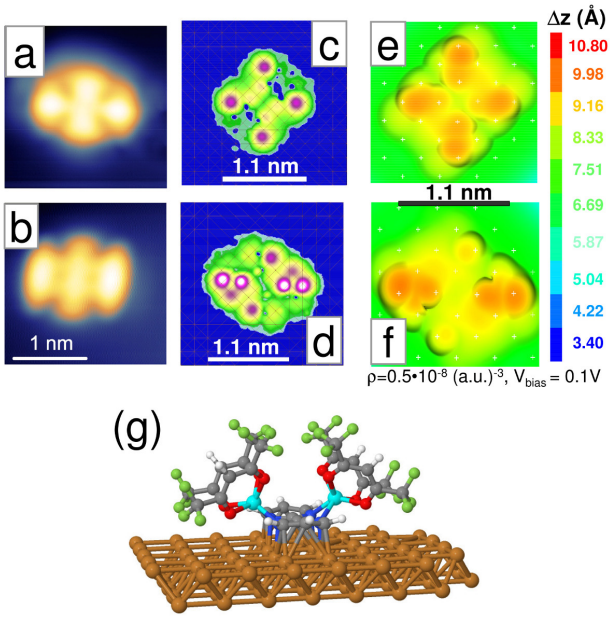


FIG. 6. Experimentally recorded (a,b) Ni_2-β and simulated STM images of the Ni_2 complex, with partially weakened chemical bonds, bound to Cu(001) via the bpym moiety (see lower plot). Theoretical images are computed with VASP[47](c,d) and AITRANSS[49] (e,f). Images (c) and (e) are obtained assuming symmetry constrains within the DFT relaxation procedure, while images (d) and (f) correspond to the relaxed structure without constrains (see text for further details). Lower plot shows distorted Ni_2 complex with partially weakened chemical bonds is bound to Cu(001) via (bpym) moiety.

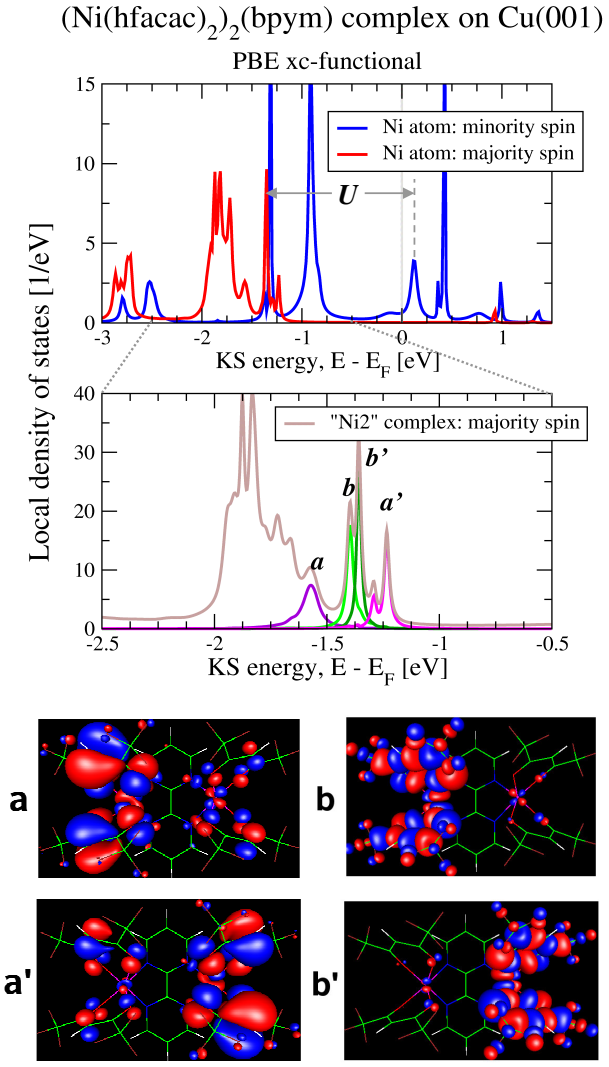


FIG. 7. Upper plot: spin-dependent local density of states projected on one of Ni atoms of the distorted Ni_2 complex deposited on Cu(001) [for a geometrical arrangement, see Fig. 6g]. Middle (zoomed in) plot shows majority (up-) spin spectral function below the Fermi-level, where contributions are highlighted arising from four orbitals (a, b, a' and b'), each carrying one unpaired spin. Corresponding wave functions are presented below. There a and b are localized on the "left-hand" side, while a' and b' are localized on the "right-hand" side of the molecular complex.

Assuming that the weak AF coupling between the two subsystems is below the Kondo-temperature, $J_{AF} = (E_{AF} - E_F)/2 \simeq 12\text{K} \leq T_K$ (otherwise the AF singlet ground state would be incompatible with the Kondo-effect observed experimentally), each subsystem will undergo Kondo-screening independently below the Kondo-temperature. We note that due to inversion center, each

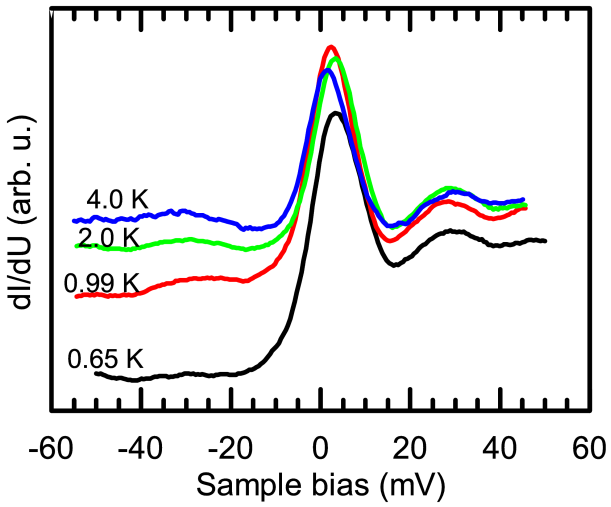


FIG. 8. Differential conductance dI/dU of Ni_2-β measured at different temperatures. Sidebands at 30 mV are surrounding the Kondo-resonance at zero bias. Feedback conditions: U = 50 mV, I = 1 nA, 2 mV modulation.

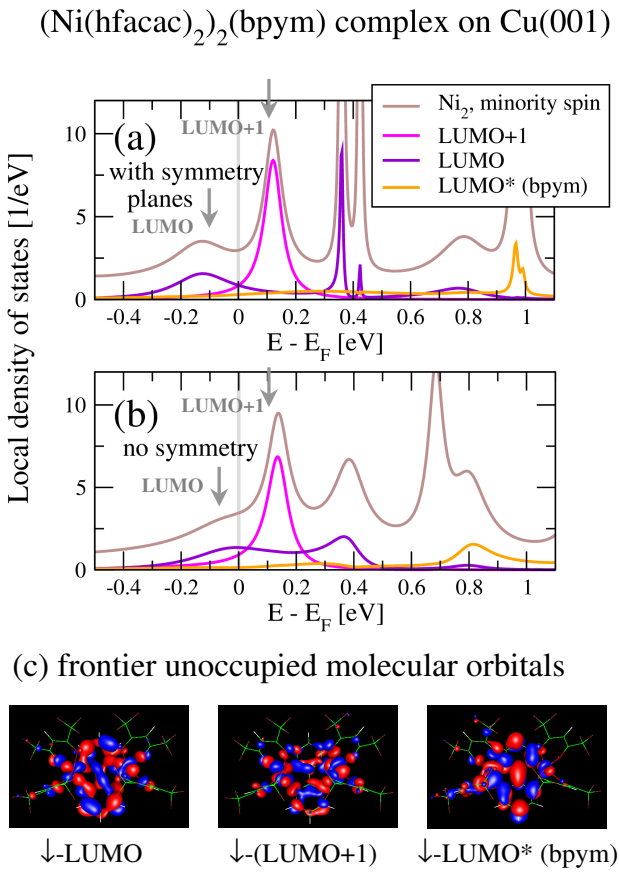


FIG. 9. (a) and (b) Kohn-Sham spectral function of Ni_2 complex at Cu surface in the minority spin channel; panel (a): Ni_2 complex with local C_{2v} symmetry; panel (b): Ni_2 complex relaxed at surface without symmetry constrains. Lower plot (c) shows frontier (minority-spin) unoccupied molecular orbitals.

spin has its own conduction channel[53]. Using equation (4) (limit $U \gg \varepsilon_d$), and parameters read from the computed spectral function (see Fig. 7),

$$2\Gamma^* = \Gamma_{a,a'} \simeq 0.1 \text{ eV} \gg \Gamma_{b,b'},$$
$$\varepsilon_d \sim 0.06 \div 0.125 \text{ eV}, \quad U \simeq 1.5 \text{ eV} \gg \varepsilon_d,$$

we estimate $T_K \sim 0.4 \div 20$ K, where the upper limit is above J_{AF} and is in the range of experimental values.

D. Satellites accompanying the Kondo-resonance

Yet another intriguing experimental observation, found in the differential conductance dI/dU of Ni_2-β, are two satellites at ± 30 mV (Fig. 8). We discuss further four possible hypotheses, which might explain their origin. These are: (a) parallel conduction through frontier molecular orbitals (LUMOs); (b) low-energy magnetic excitations from the singlet ground state within the binuclear complex; (c) zero-field splitting of the triplet state of Ni^{2+} ion; and (d) low-energy vibrational excitations of the complex and associated with that phonon-assisted Kondo-effect. According to the analysis presented below, three hypotheses (a), (b) and (c) are likely to be ruled out in favor of the hypothesis (d).

Hypothesis (a). The first plausible suggestion is that satellites in dI/dU around the Kondo-resonance may be attributed to the parallel conduction through the LUMO and LUMO+1 of a Ni_2 complex, as summarized in Fig. 9. A distorted gas-phase Ni_2 complex has almost degenerate LUMO and LUMO+1 levels (e.g., in the minority spin channel, if Ni spins are coupled ferromagnetically), with splitting $\Delta \simeq 0.08$ eV comparable with the required energy scale $2\,\delta E \simeq 0.06$ eV. A pair of LUMO and LUMO+1 wave functions (see Fig. 9c) involve d-orbitals of two Ni^{2+} centers hybridized via π-states of the central bpym-unit. When the Ni_2 complex is deposited on a Cu surface (Fig. 6), the molecular orbitals hybridize with the substrate states in different ways,[54] as seen from Figs. 9a,b. Two "satellites" are seen in the DFT spectral function $A(E)$: below E_F (a "shoulder" of the partially occupied LUMO state) and above E_F (mainly, LUMO+1 resonance).[57] However, these "satellites" are placed at energies around ± 100 meV *vs* the Fermi-level, i.e. above the required energy $\delta E \simeq 30$ meV. Their positions in the spectral function $A(E)$ are furthermore sensitive to the variations in the absorption geometry (cf. plots a and b in Fig. 9), and it is unlikely that the found "satellites" are always expected at equidistant points with respect to the Fermi-level.

Hypothesis (b). Following the data presented in Table I, also magnetic excitations are unlikely to be the cause. A transition from AF to F coupling of S=1 spins

happens at the energy scale ~ 2 meV, too small to explain peaks at ± 30 meV. Furthermore, the AF singlet ground state is not compatible with the observed Kondo-effect. Furthermore, breaking Hund's rule and flipping a 1/2 spin at the Ni^{2+} center is too expensive (~ 0.5 eV, see Table I).

Hypothesis (c) relies on zero-field spitting of a triplet S=1 state (we refer here to one of the magnetically almost isolated subsystem — a $Ni(hfacac)_2$ unit with a single Ni^{2+} center). Because of spin-orbit interaction, the triplet splits into a (quasi-degenerate) doublet and a singlet, with the lowest energy state to be depended on the sign of the largest anisotropy constant D in the zero-field spin Hamiltonian, $H_{ZF} = D[S_z^2 - S(S+1)/3] + E(S_x^2 - S_y^2)$. An experimental evidence exists, Ref. 58, that for example under a strong distortion of the octahedral symmetry splitting can be of few meV. However, if $D > 0$, the ground state is singlet, while the doublet is accessible at non-zero bias voltages only corresponding to a split Kondo-resonance, a situation that is not observed experimentally. Contrary, if $D < 0$, the ground state is (almost) degenerate, provided $|E| \ll |D|$. At zero bias-voltage a fluctuation from $S_z = 1$ to $S_z = -1$ is not easily possible, since $\Delta S_z = 2$ is not compatible with a spin-flip event by a single substrate electron with $\Delta m = 1$. In this situation, only a scattering event of second order involving two electrons can cause a Kondo-effect, which would result in extremely low Kondo-temperatures.

Hypothesis (d). Under applied bias voltage, a "hot" electron tunneling from the STM-tip (or from the surface) through a molecule may release its energy via emitting a phonon before participating in the spin-flip scattering processes. Such an inelastic Kondo-effect would manifest as a "copy" of the Kondo-resonance in dI/dU, which is, however, shifted from zero bias to the energy of molecular vibration[59].

To verify this idea, we have performed quantum-chemistry calculations of the electron-phonon coupling matrix elements for the Ni_2 complex. To simplify our analysis, we have considered a distorted molecular conformation of Ni_2 with imposed C_{2v} symmetry that closely resembles the atomic structure of the complex pre-optimized nearby a Cu(001) surface (see Suppl. Figs. 1b and 4a in Supplementary Information[31]).

To first order, molecular vibrations of two $Ni(hfacac)_2$ units can be considered independently, since these units are attached to the bpym-moiety, which is strongly bound to the Cu surface. Therefore, we consider one of the $Ni(hfacac)_2$ units and define an "active" subspace limited to 15 atoms including one Ni^{2+} ion and surrounding atoms in its vicinity (see Fig. 10). There "colored" atoms are allowed to vibrate, while all other "reservoir" atoms shown in gray are assumed (as an approximation) to have infinite masses: either because some of them are heavy trifluoromethyl CF_3 groups, or because other atoms are bound to the surface. Such an approximation provide us with a set of 45 well-defined vibrational frequencies ω_μ.

Further, we consider the wave function ψ_K (Fig. 10b),

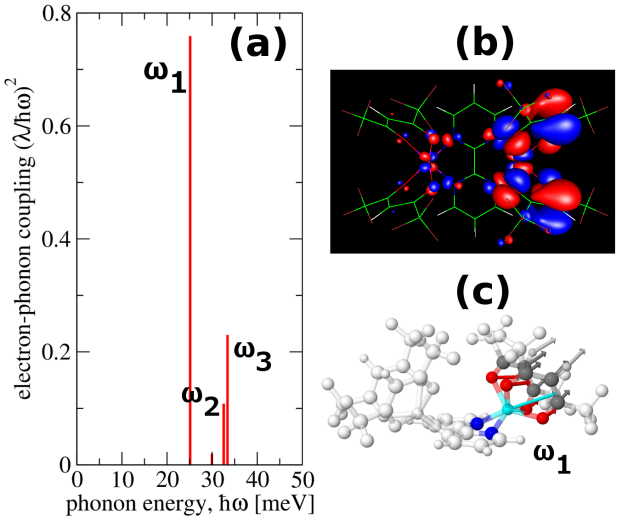


FIG. 10. Dimensionless electron-phonon (*el-ph*) coupling constants, plot (a), between the "Kondo-active" molecular orbital ψ_K shown in plot (b) and low-energy vibrational eigenmodes, which are forced to be localized in the vicinity of Ni^{2+} ion at the right-hand side of the molecule (see text for details). Plot (c) is a visual representation of the mode (atomic displacements are scaled by $\times 10$) with energy $\hbar\omega_1 = 25.1$ meV exhibiting the largest *el-ph* coupling constant ≈ 0.75.

which dominates in the scattering channel responsible for the Kondo-effect (essentially, ψ_K is one of those single-occupied molecular orbitals depicted as a and a' in Fig. 9, which strongly hybridize with the Cu surface)[60]. We have computed electron-phonon coupling matrix elements λ^μ, involving the orbital ψ_K and molecular vibrations, which are localized within the same "active" subspace (for computational details, see Supplementary Information,[31] Sec. III).

Our results are presented in Fig. 10 in which we show the dimensionless electron-phonon coupling constants $g = (\lambda^\mu/\hbar\omega_\mu)^2$ limited to the low-energy excitations. We observe only three eigenmodes (25.1 meV, 32.6 meV and 33.4 meV) with non-zero coupling constants and frequencies in the proximity of $\delta E \simeq 30$ meV. Furthermore, we show in the Supplementary Information,[31] Sec. III, that the eigenmodes involve vibrations of Ni^{2+} ions. Their energies will be renormalized when coupled to a continuum of vibrational modes of the macroscopic system, including remaining functional groups of the molecular complex and the Cu surface. However, our additional calculations show that, for example, interaction between two Ni-subsystems introduces a moderate splitting of the frequencies only, around ~ 0.5 meV. Thus, we argue that three vibrational eigenmodes may rationalize the observation of satellites in dI/dU as a signature of the phonon-assisted Kondo-effect.

V. CONCLUSION

To summarize, low temperature STS measurements on binuclear metal-organic complexes, "Ni_2" and "Mn_2", deposited on a Cu(001) surface revealed that the systems undergo the Kondo-effect with the Kondo-resonances located nearby transition metal atoms. The relatively large Kondo-temperatures, of the order of ~ 10 K, were found to depend on the adsorption-type. The situation was intriguing here, because the synthesized molecules do not have predefined anchoring groups, which could be responsible for a formation of the chemical bond with the Cu surface.[22]

We rationalized experimental observations by performing extensive density functional theory calculations. We searched for the adsorption geometries, where molecules are chemisorbed on the surfaces. In case of "Ni_2", our simulations show that some STM images (Ni_2-β) can be attributed to a distorted "Ni_2" complex with partially weakened internal chemical bonds, while other STM images (Ni_2-α) may be interpreted as arising from molecular fragmentation. In both cases, our calculations suggest a picture of the underscreened (S=1)-type Kondo-effect emerging from the open $3d$ shells of the individual Ni^{2+} ions. Furthermore, theoretical analysis points out that the satellites in the STS spectra observed nearby the zero-bias resonance are likely a signature of the low-energy vibrational excitations of the "Ni_2" complex and associated with that phonon-assisted Kondo-effect.

In broader terms, binuclear complexes present an excellent playground for studying fundamental aspects of magnetic two-impurity (or double quantum dot) systems. By functionalizing the bridging unit it could be possible to enhance the super-exchange interaction between two centers, thus allowing to access different regions of the phase diagram of the double impurity model[53,61,62]. On the applied level, understanding interaction between the spins residing on different functional units is vital to quantum information storage and processing with molecules assembled on surfaces. Our work provides an important step in this direction and identifies further challenges. Apart from the appealing enhancement of the super-exchange, the substitution of Ising-like spins (such as Tb) may offer means to study a "double molecular magnet". As demonstrated here, first-principles calculations will play an indispensable role in this effort.

ACKNOWLEDGMENTS

We thank Karin Fink for fruitful discussions and Marius Bürkle for providing us with a development version of the TURBOMOLE package. A.B. acknowledges support of DFG through the research grant BA 4265/2-1. W.W. and M.R. acknowledge support from the Baden-Württemberg Stiftung in the framework of the Kompetenznetz für Funktionale Nanostrukturen (KFN).

[1] J. Reichert, R. Ochs, D. Beckmann, H. B. Weber, M. Mayor, and H. v. Löhneysen, Phys. Rev. Lett. **88**, 176804 (2002).
[2] M. Elbing, R. Ochs, M. Koentopp, M. Fischer, C. von Hänisch, F. Weigend, F. Evers, H. B. Weber, and M. Mayor, Proc. Natl. Acad. Sci. USA **102**, 88158820 (2005).
[3] J. Park, A. N. Pasupathy, J. I. Goldsmith, C. Chang, Y. Yaish, J. R. Petta, M. Rinkoski, J. P. Sethna, H. D. Abruña, P. L. McEuen, and D. C. Ralph, Nature **417**, 722 (2002).
[4] S. Kubatkin, A. Danilov, M. Hjort, H. Cornil, J.-L. Brédas, N. Stuhr-Hansen, P. Hedegård, and T. Bjørnholm, Nature **425**, 698 (2003).
[5] E. A. Osorio, K. O'Neill, N. Stuhr-Hansen, F. Nielsen, T. Bjørnholm, H. S. J. van der Zant, Adv. Materials, **19**, 281285 (2007).
[6] E. Lörtscher, J. W. Ciszek, J. Tour, H. Riel, Small **2**, 973977 (2006).
[7] V. Meded, A. Bagrets, A. Arnold, and F. Evers. Small **5**, 2218-2223 (2009).
[8] S. Schmaus, A. Bagrets, Y. Nahas, T. K. Yamada, A. Bork, M. Bowen, E. Beaurepaire, F. Evers, and W. Wulfhekel, Nature Nanotech. **6**, 185-189 (2011).
[9] A. Bagrets, S. Schmaus, A. Jaafar, D. Kramczynski, T. K. Yamada, M. Alouani, W. Wulfhekel, and F. Evers. Nano Lett. **12**, 5131-5136 (2012).
[10] P. Gütlich, Y. Garcia, and H. A. Goodwinb Chem. Soc. Rev. **29**, 419-427 (2000).
[11] V. Meded, A. Bagrets, K. Fink, R. Chandrasekar, M. Ruben, F. Evers, A. Bernand-Mantel, J. S. Seldenthuis, A. Beukman, and H. S. J. van der Zant, Phys. Rev. B **83**, 245415 (2011).
[12] N. Knorr, M. A. Schneider, L. Diekhöner, P. Wahl, and K. Kern, Phys. Rev. Lett. **88**, 096804 (2002).
[13] N. Néel, J. Kröger, L. Limot, K. Palotas, W. A. Hofer, and R. Berndt, Phys. Rev. Lett. **98**, 016801 (2007).
[14] T. Jamneala, V. Madhavan, W. Chen, and M. F. Crommie, Phys. Rev. B **61**, 9990 (2000).
[15] L. Gao, W. Ji, Y. B. Hu, *et al.* Phys. Rev. Lett. **99**, 106402 (2007).
[16] Ying-Shuang Fu, Shuai-Hua Ji, Xi Chen, *et al.* Phys. Rev. Lett. **99**, 256601 (2007)
[17] I. Fernández-Torrente, K. J. Franke, and J. I. Pascual, Phys. Rev. Lett. **101**, 217203 (2008)
[18] U. G. E. Perera, H. J. Kulik, V. Iancu, L. G. G. V. Dias da Silva, S. E. Ulloa, N. Marzari, and S.-W. Hla, Phys. Rev. Lett. **105**, 106601 (2010).
[19] J. Nygård, D. H. Cobden, and P. E. Lindelof, Nature **408**, 342–346 (2000).
[20] J. Paaske, A. Rosch, P. Wölfle, N. Mason, C. M. Marcus, and J. Nygård, Nature Phys. **2**, 460–464 (2006).

[21] Single molecule magnets (SMMs) have attracted a lot of interest[23,24], recently. For example, magnetic relaxation time of SMMs could be years at low temperatures that has been observed in bulk crystals[25,26]. Potential applications of SMMs, e.g. as high-density data storage units, are envisaged. For that, individual molecular magnets need to be deposited onto supportive substrates where, due to hybridization effects, a possibility exists for surface induced changing in magnetic coupling and anisotropy.There is still a lack of clear understanding on how magnetic properties of SMMs are altered by absorption. While in the earlier studies magnetic nature of supported molecular magnets has not been demonstrated,[27] recent works on Tb(III)[28] and "Mn_{12}"-complexes[29] seem to confirm that the SMM character at the surface may be preserved.

[22] S. Wagner, F. Kisslinger, S. Ballmann, F. Schramm, R. Chandrasekar, T. Bodenstein, O. Fuhr, D. Secker, K. Fink, M. Ruben, and H. B. Weber Nat. Nanotech. **8**, 575–579 (2013).

[23] D. Gatteschi and R. Sessoli, Angew. Chem. Int. Ed. **42**, 268 (2003).

[24] L. Bogani and W. Wernsdorfer, Nature Materials **7**, 179 (2008).

[25] G. Christou, D. Gatteschi, D. N. Hendrickson, and R. Sessoli, Mater. Res. Soc. Bull. **25**, 6671 (2000).

[26] M. Cavallini, M. Facchini, C. Albonetti, and F. Biscarini, Phys. Chem. Chem. Phys. **10**, 784 (2008).

[27] J. Gómez-Segura, I. Díez-Pérez, N. Ishikawa, M. Nakano, J. Vecianaa and D. Ruiz-Molina Chem. Commun. **27**, 2866-2868 (2006).

[28] L. Vitali, S. Fabris, A. M. Conte, S. Brink, M. Ruben, S. Baroni, and K. Kern, Nano Letters **8**, 3364-3368 (2008).

[29] S. Kahle, Zh. Deng, N. Malinowski, Ch. Tonnoir, A. Forment-Aliaga, N. Thontasen, G. Rinke, D. Le, V. Turkowski, T. S. Rahman, S. Rauschenbach, M. Ternes, and K. Kern, Nano Letters **12**, 518-521 (2011).

[30] W. Liang, M. P. Shores, M. Bockrath, J. R. Long, and H. Park, Nature **417**, 725 (2002).

[31] PDF file with Supplementary Information can be found within the source file accompanying this submission.

[32] M. Barquín, M. J. G. Garmendia, and V. Bellido, Trans. Met. Chem. **24**, 546 (1999).

[33] G. Brewer and E. Sinn, Inorg. Chem. **24**, 4580 (1985).

[34] L. Zhang, T. Miyamachi, T. Tomani, R. Dehm, and W. Wulfhekel, Rev. Sci. Instrum. **82**, 103702 (2011).

[35] P. W. Anderson, Phys. Rev. **124**, 41 (1961).

[36] L. Kouwenhoven and L. Glazman, Physics World **14**, 33 (2001).

[37] U. Fano, Phys. Rev. **124**, 1866 (1961).

[38] O. Újsághy, J. Kroha, L. Szunyogh, and A. Zawadowski, Phys. Rev. Lett. **85**, 2557 (2000).

[39] J. Merino and O. Gunnarsson, Phys. Rev. B **69**, 115404 (2004).

[40] M. Plihal and J. W. Gadzuk, Phys. Rev. B **63**, 085404 (2001).

[41] K. Nagaoka, T. Jamneala, M. Grobis, and M. F. Crommie, Phys. Rev. Lett. **88**, 077205 (2002).

[42] V. Blum, R. Gehrke, F. Hanke, P. Havu, V. Havu, X. Ren, K. Reuter, and M. Scheffler, Comp. Phys. Comm. **180**, 2175-2196 (2009).

[43] R. Ahlrichs, *et al.* TURBOMOLE 6.6 (development version), program package for *ab initio* electronic structure calculations, Turbomole GmbH (2014).

[44] A.C. Hewson, *The Kondo Problem to Heavy Fermions* (Cambridge Studies in Magnetism, Band 2). Cambridge University Press (1993).

[45] The formula for the Kondo temperature reads as:

$$k_B T_{\rm K} \simeq 0.41U\sqrt{\frac{\Gamma}{4U}}\; e^{-\frac{\pi(U-\varepsilon_d)\varepsilon_d}{U\Gamma}},$$

where $-\varepsilon_d < 0$ is a position of the occupied resonance level measured *vs* Fermi-energy, Γ is the resonance width and U is Coulomb on-site interaction.

[46] A. Tkatchenko and M. Scheffler, Phys. Rev. Lett. **102**, 073005 (2009).

[47] G. Kresse and J. Furthmüller, Phys. Rev. B **54**, 11169 (1996).

[48] A. Arnold, F. Weigend, and F. Evers, J. Chem. Phys. **126**, 174101 (2007).

[49] J. Wilhelm, M. Walz, M. Stendel, A. Bagrets, and F. Evers, Phys. Chem. Chem. Phys. **15**, 6684 (2013).

[50] J. P. Perdew, K. Burke, and M. Ernzerhof, Phys. Rev. Lett. **77**, 3865 (1996).

[51] V. I. Anisimov, F. Aryasetiawan, A. I. Lichtenstein, J. Phys.: Condens. Matt. **9** 767 (1997).

[52] S. Kümmel, L. Kronik, Rev. Mod. Phys. **80**, 3–60 (2008).

[53] C. Jayaprakash, H. R. Krishna-murthy, and J. W. Wilkins, Phys. Rev. Lett. **47**, 737 (1981).

[54] Our calculations indicate that a fractional charge of $\approx 0.5e$ leaks out from the surface to the molecule, populating partially LUMO of Ni_2 complex and LUMO* of the bpym-moiety (see Fig. 9). Also, a magnetic moment carried by the complex is slightly reduced, from $4.0\mu_B$ (gas-phase molecule) down to $3.3\mu_B$.

[55] S. L. Dudarev, G. A. Botton, S. Y. Savrasov, C. J. Humphreys, and A. P. Sutton, Phys. Rev. B **57**, 1505 (1998).

[56] A. Bagrets, J. Chem. Theory Comput. **9**, 2801 (2013).

[57] We remind that DFT with a quasi-local XC-functional does not allow to recover a Kondo-resonance at the Fermi-level.

[58] J. J. Parks, A. R. Champagne, T. A. Costi, W. W. Shum, A. N. Pasupathy, E. Neuscamman, S. Flores-Torres, P. S. Cornaglia, A. A. Aligia, C. A. Balseiro, G. K.-L. Chan, H. D. Abruña, D. C. Ralph, Science **328**, 1370 (2010).

[59] J. Paaske, and K. Flensberg, Phys. Rev. Lett. **94**, 176801 (2005).

[60] More specifically, "Kondo-active" molecular orbitals (MOs) depicted as a and a' in Fig. 9, which are strongly coupled to the Cu surface, are well approximated by symmetric and antisymmetric combinations $\psi_K^{\pm} = \frac{1}{\sqrt{2}}(\phi_{b_1}^{\uparrow} \pm \phi_{a_2}^{\uparrow})$ of the single-occupied MOs of the distorted Ni_2 complex with C_{2v} symmetry. Here b_1 and a_2 refer to irreducible representations of the C_{2v} group, with b_1 being even and a_2 being odd with respect left-right reflection σ_v.

[61] Walter Hofstetter and Herbert Schoeller, Phys. Rev. Lett. **88**, 016803 (2001).

[62] Jakob Bork, Yong-hui Zhang, Lars Diekhöner, László Borda, Pascal Simon, Johann Kroha, Peter Wahl, and Klaus Kern, Nature Phys. **7**, 901906 (2011).